Carbohydrate Polymers 99 (2014) 166–172

Contents lists available at ScienceDirect

Carbohydrate Polymers

journal homepage: www.elsevier.com/locate/carbpol

Environmentally friendly ultrosound synthesis and antibacterial activity of cellulose/Ag/AgCl hybrids

Yan-Yan Dong[a], Fu Deng[a], Jin-Jin Zhao[b], Jing He[a], Ming-Guo Ma[a,*], Feng Xu[a], Run-Cang Sun[a,c]

[a] Beijing Key Laboratory of Lignocellulosic Chemistry, College of Materials Science and Technology, Beijing Forestry University, Beijing 100083, PR China
[b] School of Materials Science and Engineering, Shijiazhuang Tiedao University, Shijiazhuang 050043, PR China
[c] State Key Laboratory of Pulp and Paper Engineering, South China University of Technology, Guangzhou 510640, PR China

ARTICLE INFO

Article history:
Received 1 July 2013
Received in revised form 11 August 2013
Accepted 14 August 2013
Available online 23 August 2013

Keywords:
Hybrids
Cellulose
AgCl
Ag
Ultrasound
Antimicrobial activity

ABSTRACT

This study aims to investigate the fabrication and property of cellulose/Ag/AgCl hybrids. In this article, preparation of cellulose/Ag/AgCl hybrids was reported using the cellulose solution, $AgNO_3$, $AlCl_3{\cdot}6H_2O$ with ultrasound agitation method. The cellulose solution was synthesized by the dissolution of the microcrystalline cellulose in NaOH/urea aqueous solution. Influences of the experimental parameters of ultrasound treatment time and ultrasonic intermittent on the hybrids were investigated. The phase, microstructure, thermal stability, and morphology of the hybrids were characterized by X-ray powder diffraction (XRD), Fourier transform infrared (FTIR) spectrometry, thermogravimetric analysis (TGA), differential thermal analysis (DTA), and scanning electron microscopy (SEM). Results showed the successful synthesis of cellulose/Ag/AgCl hybrids with good thermal stability. Moreover, the hybrids displayed desirable antimicrobial activities. Compared with other conventional methods, the rapid, green, and environmentally friendly ultrasound agitation method opens a new window to the high value-added applications of biomass.

1. Introduction

As a green method, ultrasound agitation has been receiving more and more attentions due to its many important applications in organic synthesis, materials and organometallic chemistry, and industrial manufacturing process (Mason & Lorimer, 2010; Shchukin, Radziuk, & Mohwald, 2010; Yang, Zhu, Tong, & Wang, 2007). With the help of ultrasonic irradiation, the production and modification of hybrids can be completed without high temperatures, high pressures, and long reaction times (Bang & Suslick, 2010; Suslick & Flannigan, 2007). Furthermore, ultrasound agitation is also applied in biomedical field (Ferrara, Pollard, & Borden, 2007; Gao, Fain, & Rapoport, 2005; Ng & Liu, 2002), dairy processing (Liu, Chi, Yang, & Xu, 2006), and food industry (Chemat & Khan, 2011; Knorr, Zenker, Heinz, & Lee, 2004; Patist & Bates, 2008; Zheng & Sun, 2007). The most notable effects of ultrasound agitation are consequences of acoustic cavitation (the formation, growth, and implosive collapse of bubbles), which can be categorized as primary sonochemistry (gas-phase chemistry occurring outside the bubbles) and physical modifications (caused by high-speed jets or shock waves derived from bubble collapse). These conditions are distinct from other conventional synthetic techniques such as photochemistry, wet chemistry, hydrothermal synthesis, and flame pyrolysis (Xu, Zeiger, & Suslick, 2013). Therefore, ultrasound agitation method has been accepted as a promising way for the synthesis of functional materials. During the last two decades, ultrasound agitation method has been widely applied to synthesize various functional materials, such as grapheme (Shen, Zhai, Lu, Wang, & Zheng, 2012), porous platinum electrodes (Kloke, Stetten, Zengerle, & Kerzenmacher, 2011), hollow BaF_2 nanonest (Geng, Jiang, Lu, & Zhu, 2011), Ag nanoclusters (Xu & Suslick, 2010), CdSe and CdS nanoparticles (Li et al., 2003), and gold nanoparticles (Okitsu, Ashokkumar, & Grieser, 2005).

Cellulose-based hybrids have the synergetic effect from biopolymers and inorganic materials (Olsson et al., 2010), and provide the possibility for the enhancement of multifunctional properties (Eichhorn, Dufresne, & Aranguren, 2010). According to the previous study, magnetic bacterial cellulose/Ag hybrids with high antimicrobial activity were obtained using polydopamine as a reducing agent and stabilizer (Sureshkumar, Siswanto, & Lee, 2010). Cellulose/AgCl hybrids with excellent antimicrobial activity were synthesized using cellulose solution and $AgNO_3$ in N,N-dimethylacetamide solvent (Li et al., 2012). Cellulose/$CaCO_3$ hybrids with good biocompatibility were synthesized using cellulose, $CaCl_2$, and Na_2CO_3 in ethylene glycol (Fu, Dong, Ma, Li, & Sun, 2013). Bacterial cellulose/hydroxyapatite hybrids with a 3-dimensional network were

* Corresponding author. Tel.: +86 10 62336592; fax: +86 10 62336903.
E-mail address: mg_ma@bjfu.edu.cn (M.-G. Ma).

0144-8617/$ – see front matter © 2013 Elsevier Ltd. All rights reserved.
http://dx.doi.org/10.1016/j.carbpol.2013.08.023

fabricated by a biomimetic process (Wan et al., 2006). As a photosensitive material, AgCl/Ag hybrids exhibit high photocatalytic activities and good reusability for decomposing organic pollutants such as methyl orange, rhodamine B, and methyl blue under the irradiation of common fluorescent lamp or direct sunlight (Dong, Liang, & Gong, 2012). Until now, many efforts have been placed on the synthesis of the AgCl-based hybrids (Hu et al., 2009), such as the AgCl/Ag nanocubes with high visible-light-driven photocatalytic performance was successfully synthesized by a sonochemical process (Chen, Yoo, & Huang, 2012; Li et al., 2007). Silver is well-known for its excellent antibacterial activities against bacteria and other microorganisms and has been utilized for the antibacterial applications for thousands of years (Hong, Park, Sul, Youk, & Kang, 2006; Maria et al., 2009; Pinto et al., 2009; Sharma, Yngard, & Lin, 2009). Recently, the AgCl/Ag hybrids were reported to display good antibacterial properties on *Escherichia coli*, *Staphylococcus aureus*, and *Bacillus subtilis* (Dong et al., 2012). In the previous study, our group discovered that the cellulose/Ag/AgCl hybrids had better antimicrobial activity, compared with cellulose/Ag hybrids (Li et al., 2011). The detail formation of the cellulose/Ag/AgCl hybrids needs to be further explored. However, there have been only few reports on the research of cellulose/Ag/AgCl hybrids. For example, Liu, Yang, Wang, Shi, and Jiang (2012) fabricated the antimicrobial bacterial cellulose/Ag/AgCl hybrids by using Gluconacetobacter xylinum as a versatile biofactory.

Herein, we report an ultrasound agitation method for the synthesis of cellulose/Ag/AgCl hybrids using cellulose solution, $AgNO_3$, and $AlCl_3{\cdot}6H_2O$ in NaOH/urea solvent. The microcrystalline cellulose was firstly dissoluted in NaOH/urea aqueous solution in order to form dispersed cellulose solution. As is known, NaOH/urea aqueous solution is an excellent solvent system to dissolve cellulose (Cai, Liu, & Zhang, 2006). It is very important to synthesize the hybrids with inorganic materials homogeneously dispersed within the cellulose matrix. Based on the chemical and physical effects of high intensity ultrasound, hybrids with AgCl/Ag nanoparticles dispersed homogeneously in the cellulose matrix were obtained. Furthermore, the cellulose/Ag/AgCl hybrids displayed a good thermal stability and a desirable antimicrobial activity. In the literature, a "biologic" route to fabricate bacterial cellulose/Ag/AgCl nanocomposite is reported by using microorganism for 72–168 h (Liu et al., 2012). In the present study, microcrystalline cellulose/Ag/AgCl hybrids were obtained by a rapid, green, and environmentally friendly ultrasound agitation method for 10–35 min.

2. Experimental

2.1. Preparation of hybrids from cellulose, Ag, and AgCl

All chemical materials and solvents used in the experiments were analytical grade reagents, and were used without further purification. All experiments were conducted under air atmosphere. Cellulose solution was prepared as previously described in the literature (Jia, Li, Ma, Sun, & Zhu, 2010). In a typical synthesis, a solution with NaOH/urea/H_2O of 7:12:81 by weight was prepared. Then microcrystalline cellulose (MCC, 3.24 g) was immediately dispersed into the solvent system (100 mL) under vigorous stirring, and then the suspension solution was cooled to −12 °C for 12 h.

For the synthesis of cellulose/Ag/AgCl hybrids, $AgNO_3$ (0.17 g), $AlCl_3{\cdot}6H_2O$ (0.24 g), and deionized water (30 mL) were added into the above cellulose solution (10 mL) under vigrous stirring. The above solution was subjected to sonication (Xin-Zhi, JY92-2D, Ti-horn, 20 kHz, 80 W/cm^2) at ambient condition with a high-density ultrasonic probe immersed directly in the solution. During the ultrasonic irradiation, the reaction time was 10, 15, 20, 25, 30, and 35 min, respectively. The as-prepared products were separated from the solution by centrifugation, washed with deionized water and absolute ethanol several times and dried at 60 °C in air for further characterization.

Moreover, the effect of cellulose on the products was also investigated, the sample was prepared using the mixture of $AgNO_3$, $AlCl_3{\cdot}6H_2O$, and NaOH/urea aqueous solution (7:12 in wt%, 10 mL, without MCC) by ultrosound agitation method, and kept the other conditions the same.

2.2. Characterization

X-ray powder diffraction (XRD) patterns were performed in 2θ range from 10 to 70° on a Rigaku D/Max 2200-PC diffractometer with Cu Kα radiation (λ = 0.15418 nm) and graphite monochromator at ambient temperature. Fourier transform infrared (FTIR) spectra of the cellulose/Ag/AgCl hybrids were taken on a Thermo Scientific Nicolet iN10 FTIR Microscope (Thermo Nicolet Corporation, Madison, WI, USA) in the range of wavenumber from 4000 to 675 cm^{-1}. The morphologies of hybrids were examined using a Hitachi 3400 N scanning electron microscopy (SEM) operating at 15 kV. All samples were Au coated prior to examination by SEM. Thermogravimetric analysis (TGA) and differential thermal analysis (DTA) were applied to test the thermal stability of samples with a STA-449F3 Luxx simultaneous TGA/DTA apparatus (Netzsch Co., Selb, Germany) at a scan rate of 10 °C min^{-1} from room temperature to 600 °C under N_2 atmosphere.

2.3. Antimicrobial activity studies

The antimicrobial activities of hybrids from cellulose, Ag, and AgCl were investigated against *E. coli* as the model Gram-negative bacteria and *S. aureus* as the model Gram-positive bacteria by the disc diffusion method. In the inhibition zone experiment, nutrient agar was poured into disposable sterilized Petri dish and solidified. Then 100 μL of *E. coli* and 100 μL of *S. aureus* were streaked over the dish and spread uniform. After that, circular pieces of the control and the test samples were gently placed on Petri dishes. This was done for both the bacterial strains (*E. coli* ATCC HB101 and *S. aureus* ATCC 25923). The hybrids from cellulose, Ag, and AgCl were cut into a disc shape with 1.4 cm diameter, sterilized by autoclaving at 120 °C for 20 min, and placed on *E. coli*-cultured and *S. aureus*-cultured agar plates, which were then incubated at 37 °C for 24 h. Finally, the inhibition zone was monitored.

3. Results and discussion

3.1. The phases, morphologies, and microstructures of hybrids

Fig. 1 shows the X-ray powder diffraction (XRD) patterns of the typical samples synthesized by ultrasound agitation method using $AgNO_3$, $AlCl_3{\cdot}6H_2O$, and cellulose solution (dissolution the MCC in NaOH/urea solution) at 90 °C for 10, 15, 20, 25, 30, and 35 min, respectively. One can see that the (1 1 1), (2 0 0), and (2 2 0) planes of crystallized Ag with a cubic structure (marked with * in Fig. 1, JCPDS 04-0783) and the other diffraction peaks were attributed to the well-crystallized AgCl with a cubic structure (JCPDS 31-1238). No obvious peaks of cellulose were observed, which might be due to the strong peak intensities of AgCl and Ag crystals. No peaks from impurities such as AlOOH or $Al(OH)_3$ were observed, too. The results of XRD indicated the successful preparation of AgCl and Ag crystals. Moreover, slight differences were observed among the XRD patterns. When the reaction times were 10, 15, and 20 min, the major phase was AgCl crystals and the minor phase was Ag crystals (Fig. 1a–c). However, when the reaction times were increased to 25, 30, and 35 min, Ag crystals was obtained as the major phase

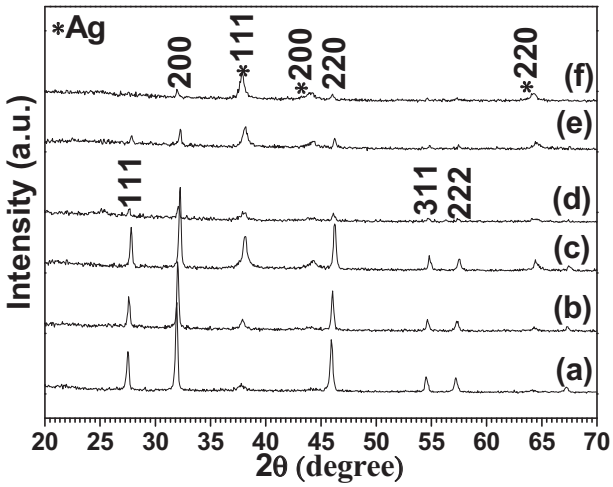

Fig. 1. XRD patterns of the cellulose/Ag/AgCl hybrids synthesized by ultrasound agitation method for (a) 10 min; (b) 15 min; (c) 20 min; (d) 25 min; (e) 30 min and (f) 35 min, respectively.

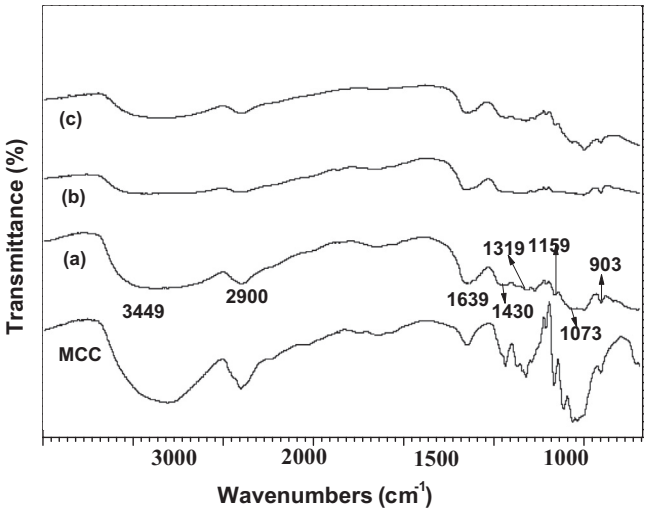

Fig. 2. FTIR spectra of pure MCC and cellulose/Ag/AgCl hybrids synthesized by ultrasound agitation method for (a) 10 min; (b) 20 min and (c) 30 min, respectively.

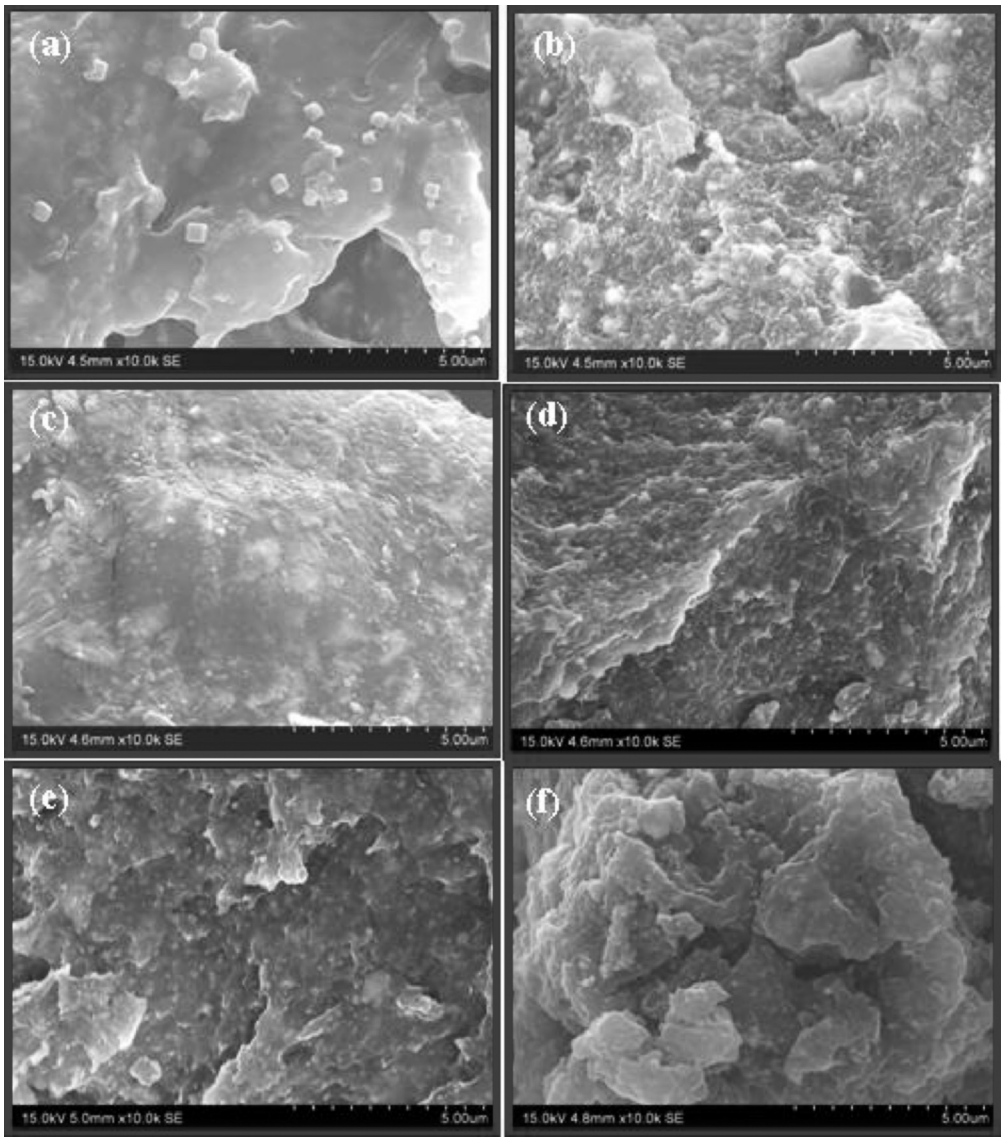

Fig. 3. SEM images of cellulose/Ag/AgCl hybrids prepared by ultrasound agitation method for (a) 10 min; (b) 15 min; (c) 20 min; (d) 25 min; (e) 30 min and (f) 35 min, respectively.

and AgCl crystals was obtained as the minor phase (Fig. 1d–f). It is also obviously to observe that the AgCl peak intensities gradually decreased and the Ag peak intensities gradually increased with the increasing reaction times. These results demonstrated that the relatively long reaction time favored for the synthesis of Ag crystals. Long reaction time favored the precipitate of cellulose, which provided a matrix for the synthesis of Ag from Ag^+. Moreover, the cellulose is a weak reducing reagent. Long reaction time maybe provides more energy for the synthesis of Ag. Of course, the intrinsic reducing procedure needs to be further explored.

As a very useful tool, FTIR has been widely used in studying functional groups of samples. Fig. 2a–c shows the FTIR spectra of the hybrids from cellulose, AgCl, and Ag by ultrasound agitation method for 10, 20, and 30 min, respectively. For comparison, the FTIR spectrum of the pure MCC was also shown in Fig. 2. The band at ~3449 cm^{-1} belongs to stretching vibration in OH group. The band at ~2900 cm^{-1} is indicative of the asymmetrical stretching vibration of C—H in pyranoid ring. The band at ~1639 cm^{-1} is attributed to the bending mode of adsorbed water. The band at ~1430 cm^{-1} is the consequence of the CH_2 bending. The adsorption band at ~1319 cm^{-1} is assigned to the C—C and C—O skeletal vibrations. The C—O antisymmetric bridge stretching exhibits a signal at ~1159 cm^{-1}. The weak peak at ~1073 cm^{-1} can be attributed to the characteristic stretching mode of the C—O in the cellulose. The band at ~903 cm^{-1} is characteristic of β-glycosidic linkages between the glucose units, which demonstrated the existence of cellulose in the products. One can observe that the peak intensities of cellulose dramatically decreased in the hybrids (Fig. 2a–c), compared with that of pure MCC, indicating the interactions between the cellulose and AgCl/Ag crystals.

The morphologies and dispersion of the hybrids were investigated by SEM. Fig. 3 shows the SEM micrographs of the samples prepared by ultrasound agitation method for 10, 15, 20, 25, 30, and 35 min, respectively. It is known that the good dispersion of inorganic nanoparticles within the cellulose matrix is important in the applications of cellulose-based hybrids (Cherian et al., 2011). When the reaction time was 10 min, one can see a few inorganic particles with cubic-like shape and size of ~50 nm were dispersed on the surface of cellulose (Fig. 3a). When the reaction time was increased to 15 min, large amounts of inorganic particles were observed and they were embedded homogenously into the cellulose matrix. However, the size of inorganic particles were dramatically decreased (Fig. 3b). When the reaction time was extended to 20 min, inorganic particles were apparently agglomerated; some of them were embedded in the cellulose matrix and some of them were dispersed on the surface of cellulose (Fig. 3c). Moreover, the size of inorganic particles synthesized for 20 min became larger than that for 15 min. No obvious differences were observed within the SEM images of samples synthesized for 25 and 30 min (Fig. 3d and e). When the reaction time was increased to 35 min, a slight decline in the number of inorganic particles occurred (Fig. 3f). From Fig. 3, one can get an overview of the changing process of inorganic particles in the hybrids.

The influences of ultrasonic intermittent on the hybrids were also investigated. The samples were prepared for 30 min with an ultrasonic intermittent at on 2 s/off 1 s, on 2 s/off 3 s, on 2 s/off 4 s, respectively. Fig. 4a–c showed the XRD patterns of the as-prepared hybrids. All the hybrids consisted of mixed phases of AgCl and Ag crystals (Fig. 4a–c). It is worth pointing out that the peak intensities of AgCl crystals were dramatically increased with the increasing off time; conversely, the peak intensity of (1 1 1) plane in Ag crystals decreased. This result demonstrated that longer off time favored the synthesis of AgCl crystals and the ultrasonic intermittent played an important role in the growth of Ag crystals. This can be assigned to the consequences of acoustic cavitation and physical modifications caused by high-speed jets and shock waves (Xu, Zeiger, & Suslick, 2013). The influence of cellulose on the phases of hybrids was explored in the paper, as was shown in Fig. 4d. One can see that the sample synthesized without MCC consisted of mixed phases of well-crystallized AgCl with a cubic structure (JCPDS 31-1238, major phase) and Ag with a cubic structure (JCPDS 04-0783, minor phase). There is only a weak peak of (1 1 1) plane in Ag crystals was observed, indicating that cellulose played an important role in the process of reducing Ag+ to metal Ag. This result is in good accord with the previous researches in the literature, which reported that cellulose has the ability to reduce metal ions (Friedrich & Taubert, 2008). It can be explained as follows, with the high temperature of ultrasound agitation, most of the β-(1,4) glycosidic linkages between the glucose units in the cellulose were broken; and then, large amounts of glucose units with plenty of reducing ends were obtained. These reducing ends can be helpful in reducing Ag+ to metal Ag. The schematic representation of the formation process of the cellulose/Ag/AgCl hybrids was shown in Fig. 5.

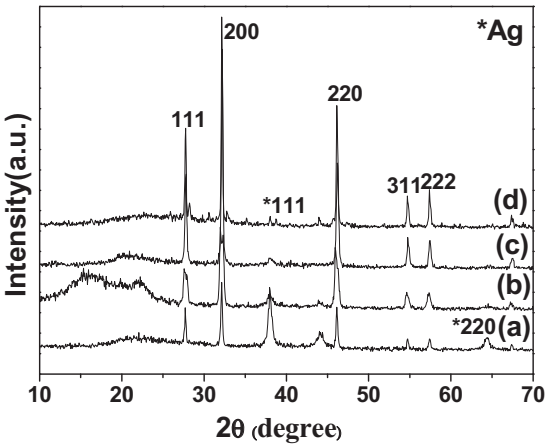

Fig. 4. XRD patterns of cellulose/Ag/AgCl hybrids synthesized by ultrasound agitation method for different intermittent: (a) on 2 s/off 1 s; (b) on 2 s/off 3 s; (c) on 2 s/off 4 s and (d) AgCl/Ag hybrids synthesized without MCC dissolution in NaOH/urea aqueous solution.

The corresponding SEM images of samples using different ultrasonic intermittent were shown in Fig. 6. When the ultrasonic intermittent off time was 1 s, inorganic particles were observed to be dispersed on the surface of cellulose (Fig. 6a). By increasing the ultrasonic intermittent off time to 2 s, one could observe that inorganic particles were embedded in the cellulose matrix clearly (Fig. 6b). When the ultrasonic intermittent off time was increased to 3 s, cellulose with block-like shape was obviously observed and one can also see inorganic particles which were dispersed on the surface of cellulose (Fig. 6c). Compared with Fig. 6c, no obvious differences were observed when the ultrasonic intermittent off time was further increased to 4 s (Fig. 6d). Based on the SEM micrographs, one can conclude that the ultrasonic interment has no significant effect on the morphology and dispersion of the as-prepared hybrids.

3.2. *The thermal stability and antibacterial activity of hybrids*

The thermal stability of the hybrids from cellulose, AgCl, and Ag was further explored with TGA and DTA. TGA and DTA curves of the cellulose/Ag/AgCl hybrids synthesized by ultrasound agitation method for 10, 20, and 35 min are shown in Fig. 7, respectively. From Fig. 7, one can observe that all the samples showed obvious weight loss from 217 to 340 °C in the TGA curves, accompanied by exothermic peaks at about 273, 279, and 305 °C in the DTA curves (Fig. 7B). This can be due to the thermal degradation and complete decomposition of cellulose in the hybrids. The total weight losses of hybrids synthesized for 10, 20, and 35 min were ~54%, ~52%, and

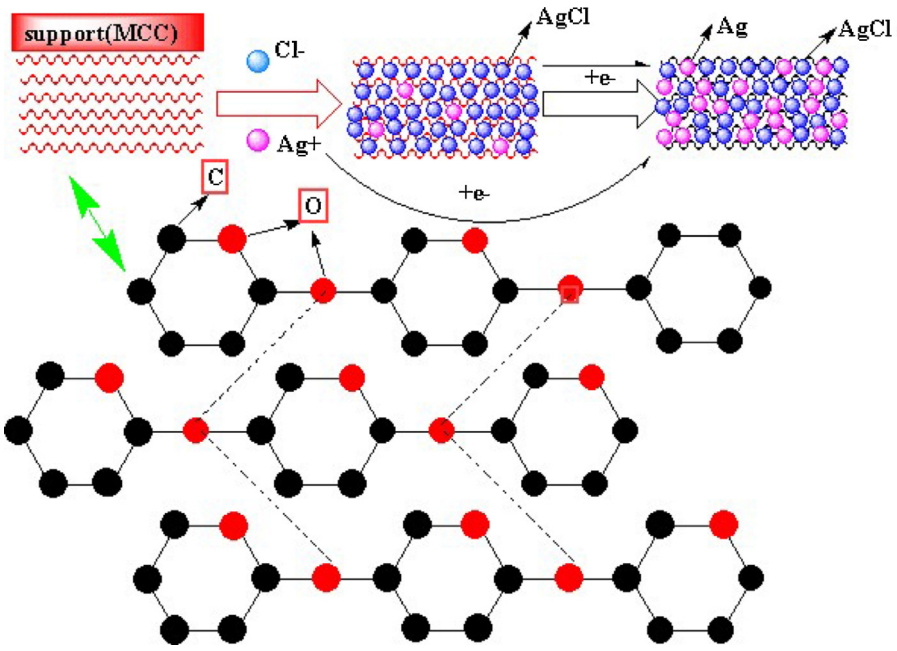

Fig. 5. Schematic representation of the formation process of the cellulose/Ag/AgCl hybrids.

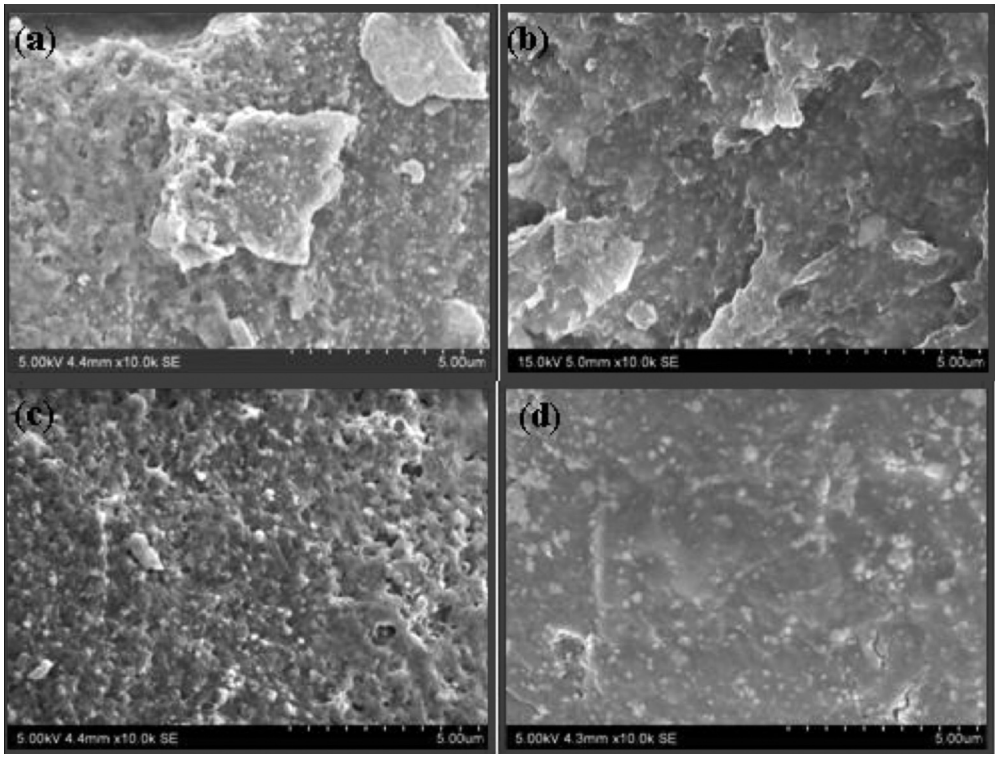

Fig. 6. SEM images of the cellulose/Ag/AgCl hybrids prepared by ultrasound agitation method for different ultrasound intermittent at: (a) on 2 s/off 1 s; (b) on 2 s/off 2 s; (c) on 2 s/off 3 s and (d) on 2 s/off 4 s.

~59% from room temperature to 600 °C in the TGA curves (Fig. 7A), respectively. One can also observe that the hybrids fabricated for 10 and 20 min had similar weight losses as well as thermal degradation temperatures. Nevertheless, the hybrids synthesized for 35 min exhibited relatively low total weight loss at ~59% and relatively high thermal degradation temperature at ~305 °C (Fig. 7c), indicating that the ultrasonic time had slight effect on the thermal stability of hybrids. Based on the results, one can conclude that cellulose/Ag/AgCl hybrids synthesized with longer reaction time had relatively high thermal stabilities. This result was due to the reaction between the cellulose and Ag/AgCl particles. Due to the thermal procedure, cellulose decomposed and residue left was Ag/AgCl particles. When the cellulose/Ag/AgCl hybrids were obtained using relatively long ultrasonic irradiation time, the concentration of Ag/AgCl particles was relatively low, inducing relatively high thermal stabilities.

The antibacterial activity of the hybrids from cellulose, AgCl, and Ag was also shown in Fig. 8. Pure MCC was used as control. From the

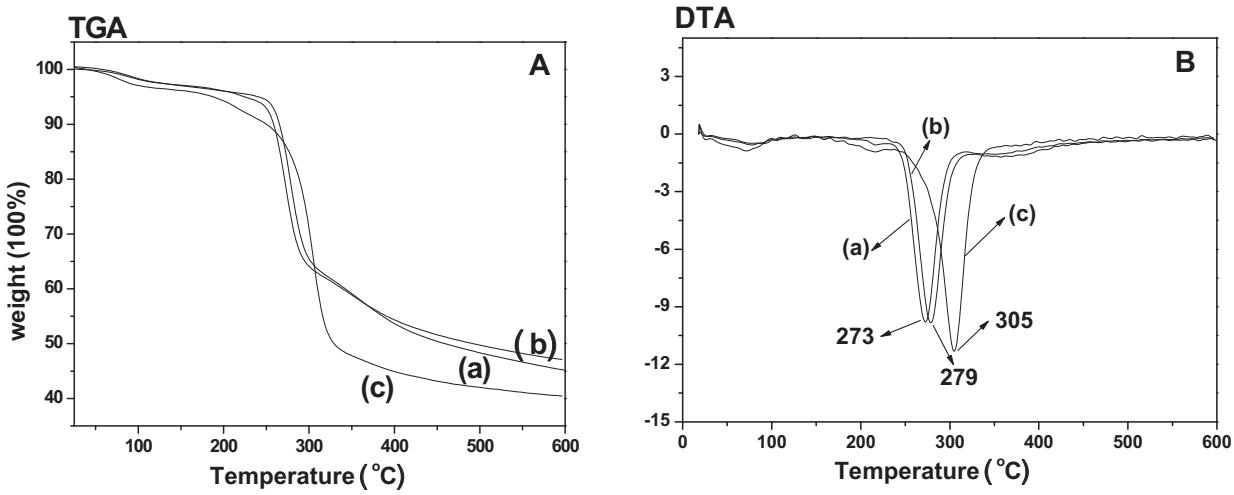

Fig. 7. TGA and DTA curves of cellulose/Ag/AgCl hybrids synthesized by ultrasound agitation method for (a) 10 min; (b) 20 min and (c) 35 min, respectively.

images of control in Fig. 8, no inhibition zone was observed, indicating that the pure MCC did not have any antimicrobial activities and that cellulose was only used as matrix for the dispersion of AgCl and Ag crystals. The inhibition zones of the sample synthesized by ultrasound agitation method for 10 min for *E. coli* and *S. aureus* were 2.0 and 3.0 mm, respectively (Fig. 8a and b). The inhibition zones of the hybrids from cellulose, AgCl and Ag synthesized by ultrasound agitation method for 30 min for *E. coli* and *S. aureus* were 2.0 and 2.5 mm, respectively (Fig. 8c and d). These results confirmed that the AgCl/Ag nanoparticles had good antimicrobial activities. Moreover, the antimicrobial activity against *E. coli* was lower than that against *S. aureus*, which might be assigned to the differences in cell walls between Gram-negative and Gram-positive bacteria (Feng et al., 2000). According to the results of antimicrobial experiments, one can conclude that the hybrids synthesized with shorter reaction time exhibited better antimicrobial activities, indicating that the ultrasonic times have slight effect on the antimicrobial activities of hybrids from cellulose, AgCl, and Ag. It is worth noting that when the samples were placed on the dishes with bacteria, some convex protrusions appeared, as shown in Fig. 8. This bulge phenomenon can be assigned to the water swelling of hybrids. Based on the results of antimicrobial activity, one can conclude that the

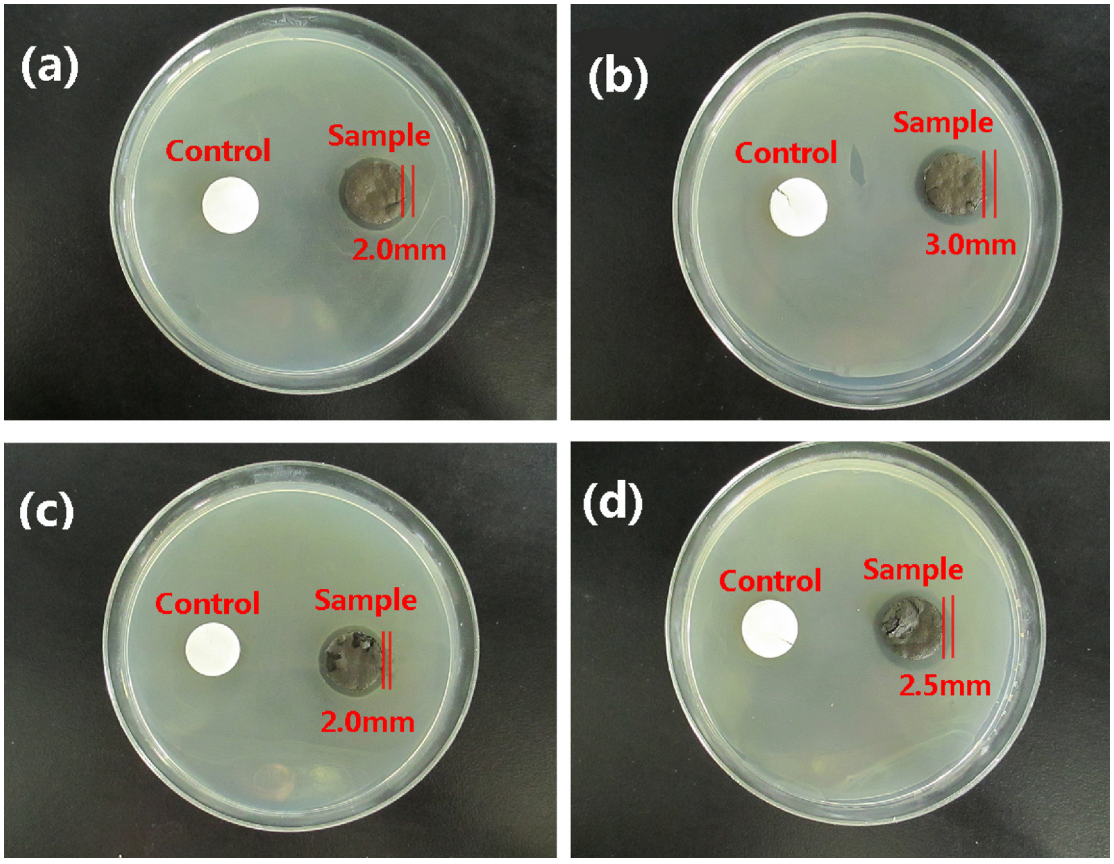

Fig. 8. Antimicrobial activities of the cellulose/Ag/AgCl hybrids synthesized for (a and b) for 10 min and (c and d) 30 min: (a and c) *E. coli* and (b and d) *S. aureus*.

hybrids from cellulose, AgCl, and Ag exhibited good antibacterial activity, which may be a promising antibacterial candidate for the applications in biomedical field and public health area.

4. Conclusions

In summary, the hybrids from cellulose, AgCl, and Ag with excellent antimicrobial properties have been successfully synthesized by the ultrasound agitation method. Experimental results indicated that the AgCl/Ag nanoparticles were dispersed in the cellulose matrix. The ultrasonic time in the preparation process had slight influence on the thermal stability of cellulose/Ag/AgCl hybrids. The cellulose/Ag/AgCl hybrids exhibited a desirable antibacterial activity against both *E. coli* (Gram-negative bacteria) and *S. aureus* (Gram-positive bacteria). These hybrids might be a promising antibacterial candidate for the applications in biomedical field and public health area. This synthetic strategy reported here opens a new window to the high value-added applications of cellulose.

Acknowledgments

Financial supported from the Fundamental Research Funds for the Central Universities (No. JC2013-3, TD2011-11), Beijing Nova Program (Z121103002512030), the Program for New Century Excellent Talents in University (NCET-11-0586), the National Natural Science Foundation of China (31070511, 51102172), and Natural Science Foundation of Hebei Province (No. E2012210015) is gratefully acknowledged.

References

Bang, J. H., & Suslick, K. S. (2010). Applications of ultrasound to the synthesis of nanostrctured materials. *Advanced Materials*, *10*, 1039–1059.
Cai, J., Liu, Y., & Zhang, L. N. (2006). Unique gelation behavior of cellulose in NaOH/urea aqueous solution. *Biomacromolecules*, *7*(1), 183–189.
Chemat, F., & Khan, M. K. (2011). Applications of ultrasound in food technology: Processing, preservation and extraction. *Ultrasonics Sonochemistry*, *4*, 831–835.
Chen, D., Yoo, S. H., & Huang, Q. (2012). Sonohemical synthesis of Ag/AgCl nanocubes and their efficient visble-light-driven photocatalytic performance. *Chemistry-A European Journal*, *17*, 5192–5200.
Cherian, B. M., Leao, A. L., Souza, S. F., Costa, L. M. M., Olyveira, G. M., Kottaisamy, M., et al. (2011). Cellulose nanocomposites with nanofibers isolated from pineapple leaf fibers for medical applications. *Carbohydrate Polymers*, *4*, 1790–1798.
Dong, L. H., Liang, D. D., & Gong, R. C. (2012). In situ photoactivated AgCl/Ag nanocomposites with enhanced visible light photocatalytic and antibacterial activity. *European Journal of Inorganic Chemistry*, *19*, 3200–3208.
Eichhorn, S. J., Dufresne, A., & Aranguren, M. (2010). Review: Current international research into cellulose nanofibers and nanocomposites. *Journal of Materials Science*, *1*, 1–33.
Feng, Q. L., Wu, J., Chen, G. Q., Cui, F. Z., Kim, T. N., & Kim, J. O. (2000). A mechanistic study of the antibacterial effect of silver ions on *Escherichia coli* and *Staphylococcus aureus*. *Journal of Biomedical Materials Research*, *52*(4), 662–668.
Ferrara, K., Pollard, R., & Borden, M. (2007). Ultrasound microbubble contrast agents: Fundamentals and application to gene and drug delivery. *Annual Review of Biomedical Engineering*, *9*, 415–447.
Friedrich, Z. L., & Taubert, A. (2008). Gold microcrystal synthesis via reduction of $HAuCl_4$ by cellulose in the ionic liquid 1-butyl-3-methylimidazolium chloride. *Journal of Materials Chemistry*, *18*, 1008–1014.
Fu, L. H., Dong, Y. Y., Ma, M. G., Li, S. M., & Sun, R. C. (2013). Compare study $CaCO_3$ crystals on the cellulose substrate by microwave-assisted method and ultrasound agitation method. *Ultrasonics Sonochemistry*, *20*, 839–845.
Gao, Z. G., Fain, H. D., & Rapoport, N. (2005). Controlled and targeted tumor chemotherapy by micellar-encapsulated drug and ultrasound. *Journal of Controlled Release*, *203–222*, 1996–2001.
Geng, J., Jiang, F., Lu, Q. A., & Zhu, J. J. (2011). Ultrasound assisted self-assembly of a BaF_2 hollow nest-like nanostructure. *CrystEngCommunity*, *13*, 2758–2763.
Hong, K. H., Park, J. L., Sul, I. H., Youk, J. H., & Kang, T. J. (2006). Preparation of antimicroial poly(vinyl alcohol) nanofibers containing silver nanoparticles. *Journal of Polymer Science Part B: Polymer Physics*, *44*, 2468–2474.
Hu, W. L., Chen, S. Y., Li, X., Shi, S. A. K., Shen, W., Zhang, X., et al. (2009). In situ synthesis of silver chloride nanoparticles into bacterial cellulose membranes. *Materials Science and Engineering C-Biomimetic and Supramolecular System*, *29*, 1216–1219.
Jia, N., Li, S. M., Ma, M. G., Sun, R. C., & Zhu, J. F. (2010). Hydrothermal synthesis and characterization of cellulose-carbonated hydroxyapatite nanocomposites in NaOH–urea aqueous solution. *Science of Advanced Materials*, *2*, 210–214.
Kloke, A., Stetten, F. V., Zengerle, R., & Kerzenmacher, S. (2011). Strategies for the fabrication of porous platinum electrodes. *Advanced Materials*, *43*, 4976–5008.
Knorr, D., Zenker, M., Heinz, V., & Lee, D. U. (2004). Applications and potential of ultrasonics in food processing. *Trends in Food Science and Technology*, *5*, 261–266.
Li, H. X., Bian, Z. F., Zhu, J., Zhang, D. Q., Li, G. S., Huo, Y. N., et al. (2007). Mesoporous titania spheres with tunable chamber structure and enhanced photocatalytic activity. *Journal of the American Chemical Society*, *129*(27), 8406–8412.
Li, S. M., Fu, L. H., Ma, M. G., Zhu, J. F., Sun, R. C., & Xu, F. (2012). Simultaneous microwave-assisted synthesis, characterization, thermal stability, and antimicrobial activity of cellulose/AgCl nanocomposites. *Biomass and Bioenergy*, *47*, 516–521.
Li, S. M., Jia, N., Zhu, J. F., Ma, M. G., Xu, F., Wang, B., et al. (2011). Rapid microwave-assisted preparation and characterization of cellulose-silver nanocomposites. *Carbohydrate Polymers*, *83*, 422–429.
Li, H. L., Zhu, Y. C., Chen, S. G., Palchik, O., Xiong, J. P., Koltypin, Y., et al. (2003). A novel ultrasound-assisted approach to the synthesis of CdSe and CdS nanoparticles. *Journal of Solid State Chemistry*, *1*, 102–110.
Liu, L., Chi, Y., Yang, Y., & Xu, N. (2006). Ultrasonic technology application in dairy processing. *China Dairy Industry*, *99*, 1664–1671.
Liu, C., Yang, D., Wang, Y. G., Shi, J. F., & Jiang, Z. Y. (2012). Fabrication of antimicrobial bacterial cellulose-Ag/AgCl nanocomposite using bacteria as versatile biofactory. *Journal of Nanoparticle Research*, *14*, 1–12.
Maria, L. C. D., Santos, A. L. C., Oliveira, P. C., Barud, H. S., Messaddeq, Y., & Ribeiro, S. J. L. (2009). Synthesis and characterization of silver nanoparticles impregnated into bacterial cellulose. *Materials Letters*, *63*, 797–799.
Mason, T. J., & Lorimer, J. P. (2010). Applied sonochemistry, the uses of power ultrasound in chemistry and processing. *Chemical Engineering and Processing*, *9*, 885–900.
Ng, K., & Liu, Y. (2002). Therapeutic ultrasound: Its application in drug delivery. *Medicinal Research Reviews*, *32*, 198–205.
Okitsu, K., Ashokkumar, M., & Grieser, F. (2005). Sonochemical synthesis of gold nanoparticles: Effects of ultrasound frequency. *The Journal of Physical Chemistry, B*, *109*(44), 20673–20675.
Olsson, R. T., Samir, M. A. S. A., Salazar-Alvarez, G., Belova, L., Strom, V., Berglund, L. A., et al. (2010). Making flexible magnetic aerogels and stiff magnetic nanopaper using cellulose nanofibers as templates. *Nature Nanotechnology*, *5*, 584–588.
Patist, A., & Bates, D. (2008). Ultrasonic innovations in the food industry: From the laboratory to commercial production. *Innovation Food Science and Emerging Technologies*, *80*, 147–154.
Pinto, R. J. B., Marques, P. A. A. P., Neto, C. P., Trindade, T., Daina, S., & Sadocco, P. (2009). Antibacterial activity of nanocomposites of silver and bacterial or vegetable cellulosic fibers. *Acta Biomaterialia*, *5*, 2279–2289.
Sharma, V. K., Yngard, R. A., & Lin, Y. (2009). Silver nanoparticles: Green synthesis and their antimicrobial activities. *Advances in Colloid and Interface Science*, *145*, 83–96.
Shchukin, D. G., Radziuk, D., & Mohwald, H. (2010). Ultrasonic fabrication of metallic nanomaterials and nanoalloys. *Annual Review of Materials Research*, *40*, 345–362.
Shen, B., Zhai, W. T., Lu, D. D., Wang, J., & Zheng, W. G. (2012). Ultrasonication-assisted direct functionalization of grapheme with macromolecules. *RSC Advances*, *2*, 4713–4719.
Sureshkumar, M., Siswanto, D. Y., & Lee, C. K. (2010). Magnetic antimicrobial nanocomposites based on bacterial cellulose and silver nanoparticles. *Journal of Materials Chemistry*, *66*, 1240–1249.
Suslick, K. S., & Flannigan, D. J. (2007). Inside a collapsing bubble: Sonoluminescence and the conditions during cavitation. *Annual Review of Physical Chemistry*, *59*, 659–683.
Wan, Y. Z., Hong, L., Jia, S. R., Huang, Y., Zhu, Y., Wang, Y. L., et al. (2006). Synthesis and characterization of hydroxyapatite-bacterial cellulose nanocomposites. *Composites Science and Technology*, *11/12*, 1825–1832.
Xu, H. X., & Suslick, K. S. (2010). Sonochemical synthesis of highly fluorescent Ag nanoclusters. *ACS Nano*, *4*(6), 3209–3214.
Xu, H. X., Zeiqer, B. W., & Suslick, K. S. (2013). Sonochemical synthesis of nanomaterials. *Chemical Society Reviews*, *42*, 2555–2567.
Yang, L. X., Zhu, Y. J., Tong, H., & Wang, W. W. (2007). Submicrocubes and highly oriented assemblies of $MnCO_3$ synthesized by ultrasound agitation method and their thermal transformation to nanoporous Mn_2O_3. *Ultrasonics Sonochemistry*, *2*, 259–265.
Zheng, L., & Sun, D. W. (2007). Innovative applications of power ultrasound during food freezing process – A review. *Trends in Food Science and Technology*, *65*, 16–23.